Proceedings World Geothermal Congress 2020+1
Reykjavik, Iceland, April - October 2021

The Utah Frontier Observatory for Research in Geothermal Energy (FORGE): A Laboratory for Characterizing, Creating and Sustaining Enhanced Geothermal Systems

Joseph Moore[1], John McLennan[2], Kristine Pankow[3], Stuart Simmons[1], Robert Podgorney[4], Philip Wannamaker[1], Clay Jones[1], and William Rickard[5]

[1]Energy & Geoscience Institute, University of Utah, Salt Lake City, Utah

[2]Department of Chemical Engineering, University of Utah, Salt Lake City, Utah

[3]University of Utah Seismograph Stations, University of Utah, Salt Lake City, Utah

[4]Idaho National Laboratory, Idaho Falls, Idaho

[5]Geothermal Research Group, Palm Desert, California

Keywords: Enhanced Geothermal Systems, Frontier Observatory for Research in Geothermal Systems, FORGE, Milford Utah

ABSTRACT

The U.S. Department of Energy's (U.S. DOE) Frontier Observatory for Research in Geothermal Energy (FORGE) is a field laboratory that provides a unique opportunity to develop and test new technologies for characterizing, creating and sustaining Enhanced Geothermal Systems (EGS) in a controlled environment.

In 2018, the U.S. DOE selected a site in south-central Utah for the FORGE laboratory. Numerous geoscientific studies have been conducted in the region since the 1970s in support of geothermal development at Roosevelt Hot Springs. A vertical scientific well, 58-32, was drilled and tested to a depth of 2290 m (7515 ft) GL in in 2017 on the FORGE site to provide additional characterization of the reservoir rocks. The well encountered a conductive thermal regime and a bottomhole temperature of 199°C (390°F). More than 2000 natural fractures were identified, but measured permeabilities are low, less than 30 microdarcies. Induced fractures indicate that the maximum horizontal stress trends NNE-SSW, consistent with geologic and well observations from the surrounding area. Approximately 45 m (147 ft) at the base of the well was left uncased. A maximum wellhead pressure of 27.6 MPa (4000 psig) at an injection rate of ~1431 L/min (~9 bpm) was measured during injection testing in September 2017. Conventional diagnostic evaluations of the data, including G function analyses, suggest that hydraulic fracturing and shearing occurred. Stress gradients ranged from 13.1-14.3 kPa/m (0.58-0.63 psi/ft) for σ_{Hmin} and 15.4-18.5 kPa (0.68-0.82 psi/ft) for σ_{Hmax}. A gradient of 25.6 kPa/m (1.13psi/ft) was calculated for σ_V.

In 2019, the 2017 openhole stimulation in well 58-32 was repeated with injection rates up to 2385 L/min (15 bpm). Two additional stimulations were conducted in the cased portion of the well; one to stimulate critically stressed fractures and the second to test noncritically stressed fractures. Breakdown of the zone spanning critically-stressed fractures occurred at a surface pressure of approximately 29.0 MPa (4200 psig). Although stimulation of the noncritically stressed fractures was interrupted by failure of the bridge plug beneath the perforated interval, microseismic data suggests stimulation of the fractures may have been initiated at a surface pressure of 45.5 MPa (6600 psig). These stimulation results support the conclusion the Mineral Mountains granitoid is an appropriate host for EGS development.

Microseismicity was monitored during the stimulations using surface and downhole instrumentation. Five seismometers and a nodal array of 150 seismic sensors were deployed on the surface. A Distributed Acoustic Sensing (DAS) cable and a string of 12 geophones were deployed in well 78-32, drilled to a depth of 998 m (3274 ft) GL. A broadband sensor and a high-temperature geophone were deployed in well 68-32, drilled to a depth of 303 m (994 ft) GL. More than 420 microseismic events were detected by the geophone string. Other instruments detected fewer events.

This paper describes the results of the testing and monitoring program

1. INTRODUCTION

Enhanced Geothermal Systems (EGS) offer the potential of bringing low-cost geothermal energy to locations that lack natural permeability. Since the late 1970's, close to a dozen EGS demonstration projects have been conducted. The results have been disappointing and none of the projects have achieved large-scale commercial levels of production. The U.S. Department of Energy's Frontier Observatory for Research in Geothermal Energy (FORGE) program was initiated to develop and test techniques for creating, sustaining and monitoring EGS reservoirs. The ultimate goal of the FORGE project is to demonstrate to the public, stakeholders and the energy industry that EGS technologies have the potential to contribute significantly to future power generation.

The FORGE program is being conducted in three phases. Phase 1 involved desktop studies of existing data from five sites within the US. In 2018, the University of Utah's Milford, Utah site was selected as the site for the FORGE laboratory. During Phase 2, well 58-32 was drilled to a total depth of 2290 m (7515 ft) GL. Injection testing has been performed on three zones in this well. The well encountered low permeability crystalline rocks at 961 m (3154 ft) GL, and a bottom hole temperature of 199°C (390°F). Two additional wells, 78-32 drilled to 998 m (3274 ft) GL and 68-32, drilled 303 m (994 ft) GL were completed as seismic monitoring holes. This paper summarizes the results of the testing and monitoring program.

2. THE UTAH FORGE SITE

The Utah FORGE site is located ~322 km (200 miles) south of Salt Lake City and 16 km (10 miles) north of Milford, a small community with a population of 1400 (Fig. 1). The FORGE site is unpopulated and covers an area of about 5 km^2 (2 sq miles^2). It is situated within Utah's Renewable Energy Corridor adjacent to a 306 MWe wind farm, a 240 MWe solar field and PacifiCorp Energy's 38 MWe Blundell geothermal plant at Roosevelt Hot Springs. Cyrq Energy's 10.5 MWe geothermal field at Thermo and a biogas facility currently producing 1.5 MWe are located approximately the same distance south of Milford. An extensive road system provides access to the site.

Scientific investigations around the FORGE site have been ongoing since the late 1970s. More than 80 shallow (<500 m) and 20 deep (>500 m) wells were drilled and logged in support of geothermal development at Roosevelt Hot Springs (Fig. 2). Recent stimulation and monitoring activities, new geological mapping, 2- and 3-D seismic reflection, gravity and geochemical surveys have significantly improved our understanding of the area (Allis et al., 2018; Gwynn at al., 2018; Hardwick et al., 2018; Jones et al., 2018; Kirby et al., 2018a, b; Miller et al., 2018, and papers in Allis and Moore, 2019).

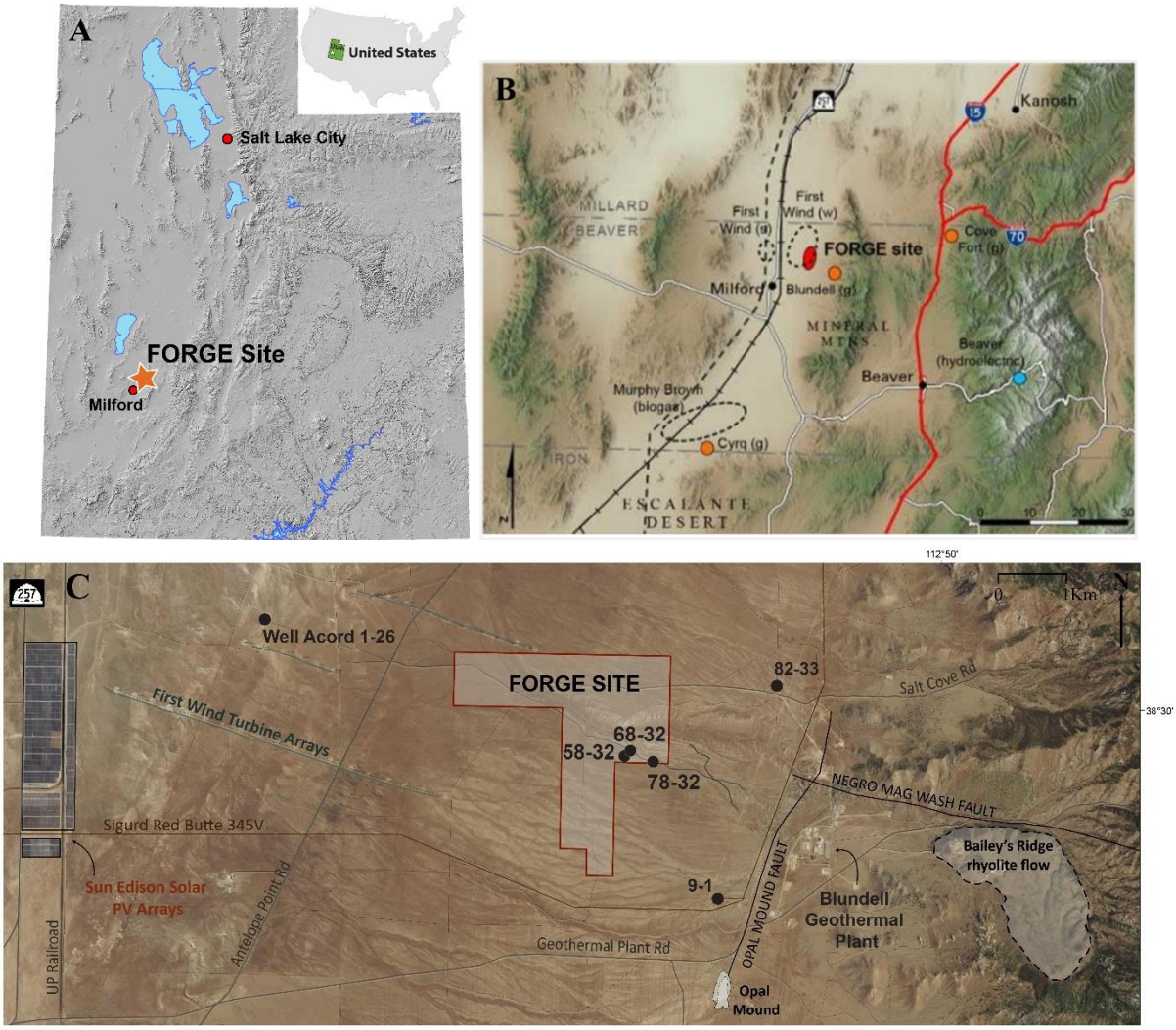

Figure 1: Location maps of the FORGE site. A) Map of Utah. B) Renewable energy projects in the region surrounding the FORGE site. Orange circles and (g) mark the locations of geothermal plants at Cove Fort, Roosevelt Springs (Blundell Power Plant and Thermo (Cyrq). Dashed ellipses show the locations of other renewable energy projects. C) Expanded view of the area immediately surrounding the FORGE site

3. GEOLOGY

The FORGE EGS reservoir will be created in Tertiary plutonic rocks that extend westward from the core of the Mineral Mountains. The pluton is composed of diorite, granodiorite, quartz monzonite, syenite, and granite (Nielson et al., 1986) (Fig. 2) ranging in age from 25.4 Ma (Aleinikoff et al., 1987) to 8 Ma (Nielson et al., 1986; Coleman and Walker, 1992). In this paper, the plutonic rocks are collectively referred to as granitoid. Quaternary (<1 My) rhyolite lava flows originating from domes along the crest of the Mineral Mountains partially cover the Precambrian gneiss exposed along the flank of the Mineral Mountains and the granitoid. Paleozoic and Mesozoic sedimentary sequences are exposed in the northern and southern parts of the Mineral Mountains but were not encountered in any of the deep wells. Temperatures of 250ºC in the Roosevelt Hot Springs reservoir suggest the presence of a still cooling magma chamber in the shallow crust.

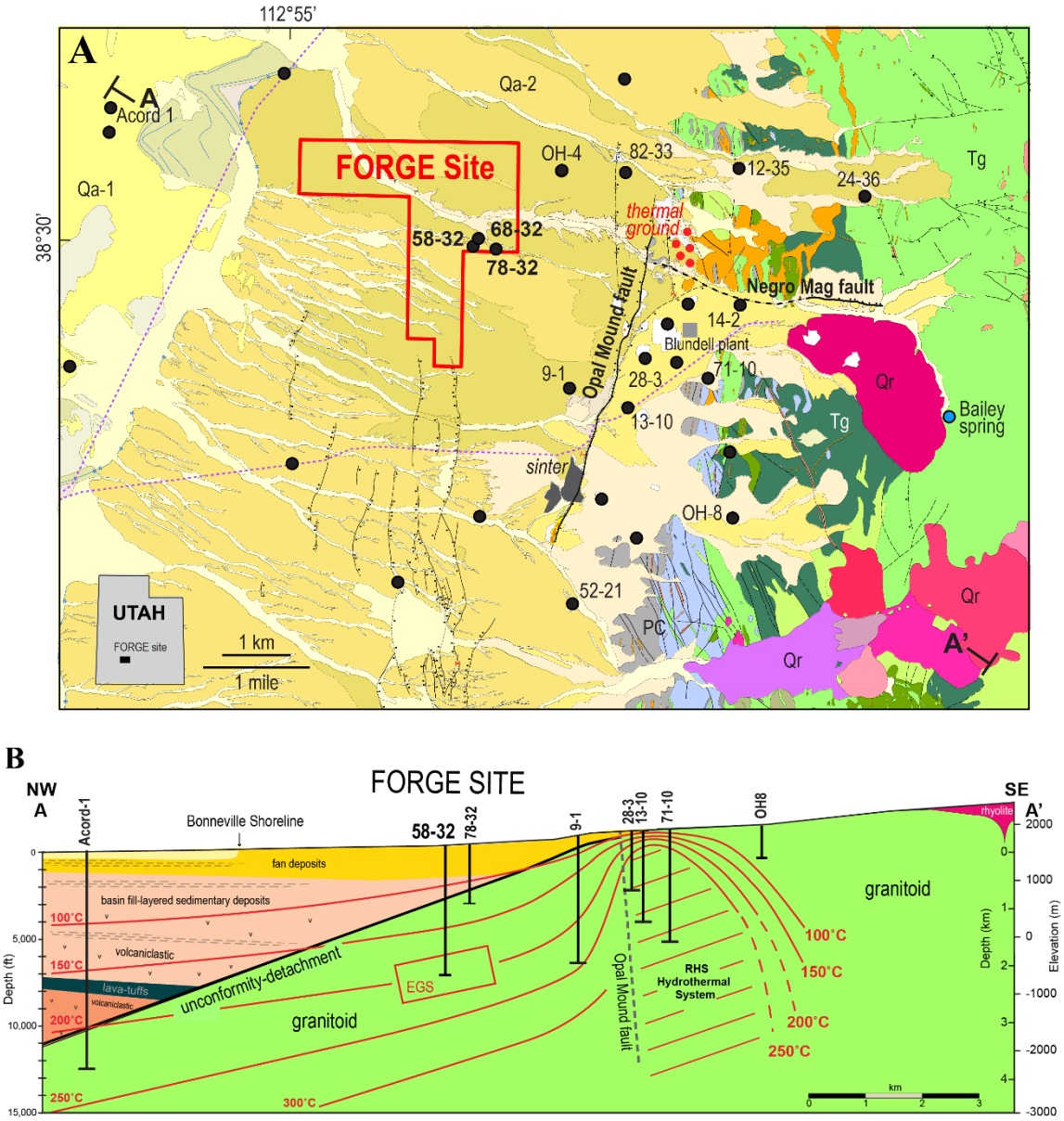

Figure 2. A) Geologic map of the FORGE site and surrounding area (modified from Nielson et al. 1986 and Kirby et al., 2018a), For clarity, only a few of the many wells are shown. Abbreviations: Qa-1=Lake Bonneville silts and sands; Qa-2=alluvial fan deposits; Qr=Quaternary rhyolite lava and pyroclastic deposits; Tg=Tertiary granitoid; PC=Precambrian gneiss; black filled circles=wells. B) Northwest-southeast section through the FORGE site showing the top of the granitoid in the vicinity of the FORGE (Kirby et al., 2018). The Roosevelt Hot Springs (RHS) geothermal system lies east of the Opal Mound fault. Isotherms are interpreted from well measurements. The red box represents the approximate position of the FORGE EGS reservoir.

Intergrown plagioclase, K-feldspar, and quartz are the dominant minerals within the granitoid (Jones et al., 2018). These minerals are accompanied by minor amounts of biotite, hornblende, clinopyroxene, apatite, titanite, zircon, and magnetite-ilmenite. Illite and chlorite are the dominant clay minerals, but they constitute <5% of the rock. Trace amounts of other secondary minerals include carbonates, anhydrite, chlorite and epidote. These hydrothermal minerals are products of paleo-geothermal activity. Granite, quartz monzonite and monzonite are the dominant lithologies encountered in well 58-32. Despite their mineralogic variations, the rocks have low permeabilities and similar mechanical properties

Acord-1, drilled to a depth of 3,855 m (12,646 ft) (Welsh, 1980), is the only deep well west of the FORGE site and the only well to penetrate deep into the basin fill of Milford Valley (Fig. 2). Acord-1 well encountered nearly 3.1 km (10,175 ft) of basin fill above the crystalline basement rocks. Poorly consolidated lacustrine and evaporite deposits characterize the basin sequence above about 1310 m (4298 ft) (Jones et al., 2018). At greater depths, Tertiary(?) tuffaceous and volcaniclastic deposits, interbedded with minor ash-flow tuffs and andesite lava flows are characteristic.

As part of the FORGE program, three new, vertical wells have been drilled to date. The deepest is well 58-32. This well was drilled to a total depth of 2288 m (7515 ft) GL. The well penetrated 961 m (3154 ft) GL of poorly sorted alluvial deposits derived from the

granitoid in the Mineral Mountains. Few fractures cut these nearly flat lying alluvial deposits. There was no evidence of ash-flow tuffs similar to those found in Acord-1. In well 58-32, the top of the basement is marked by a brecciated rhyolite interpreted to be a dike. Well 78-32, located 362 m (1187 ft) east of well 58-32 penetrated approximately 807 m (2650 ft) of alluvial deposits before encountering brecciated rhyolite at the top of the granitoid. Ultimately, this well reached a total depth of 998 m (3274.3 ft) GL and experienced a pseudo-static bottomhole temperature of 108°C. Well 68-32, located 110 m (361 ft) north of 58-32, was drilled entirely in alluvium to a depth of 303 m (994 ft) GL.

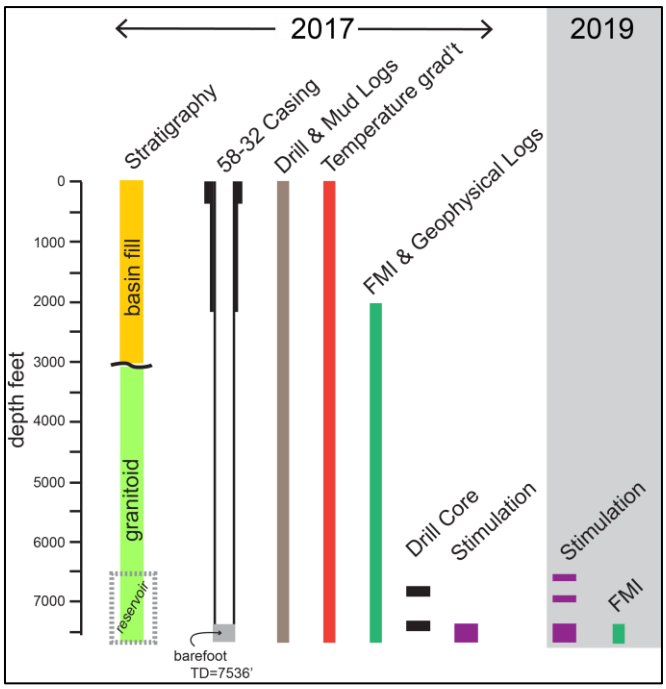

Figure 3. Summary of major activities conducted in well 58-32 in 2017 and 2019.

Structural discontinuities reflect the effects of ongoing east-west Basin and Range extension. This extension began at ~17 Ma (e.g., Hintze and Davis, 2003; Dickinson, 2006). In contrast to the steeply dipping range front faults characteristic of the Basin and Range Province, the contact between the granitoid and valley fill deposits dips approximately 20° to the west (Hardwick et al., 2016, Miller et al., 2018). Lack of deformation of the flat-lying alluvium suggests it was unconformably deposited on the granitoid. Bartley (2019) concluded, based on the orientation of dikes and fracture orientations in the Mineral Mountains, that the top of the basement represents an eroded and rotated Basin and Range fault.

The most prominent of the younger Basin and Range structures is the Opal Mound fault (Fig. 2). Temperature and pressure data demonstrate that the Opal Mound fault forms a hydraulic barrier separating the convective, permeable Roosevelt Hot Springs geothermal system from the low-permeability thermal regime to the west, beneath the FORGE site. Faults south of the Forge site form short, narrow grabens and horsts (Nielson et al., 1986; Kleber et al. 2017) that die out as the FORGE site is approached. 3-D seismic reflection surveys confirm the shallow nature of these faults (Miller et al., 2018, 2019) and the absence of any fault offsets in the granitoid-alluvial contact greater than a few 10s of meters.

The Negro Mag fault trends east-west (Fig. 2). The fault cuts across the Mineral Mountains for ~6 km. An east-west trending structure, 2 km south of the Negro Mag fault, was the site of seismicity recorded in the late 1970s (Zandt et al., 1982; Nielson et al., 1986). Both the Negro Mag and Opal Mound faults appear to terminate at their intersection.

4. STIMULATION OF 58-32

Understanding the stress directions and magnitudes is one of the essential lessons learned from past EGS projects. Despite the Mineral Mountain rotation, the current extensional regime enables assessment of the vertical and horizontal principal stress directions. At the FORGE site, the orientation of the maximum total horizontal stress, σ_{Hmax}, was inferred from the well 58-32 Formation Microscanner Image (FMI) log. More than 2000 natural fractures and 356 induced fractures were identified during logging in 2017 before running production casing (Fig. 4). Azimuths of the induced fractures indicate the orientation of σ_{Hmax} trends NNE-SSW (Fig. 4B). The same fractures were mapped in an FMI log run in the openhole section of well 58-32 after the 2019 stimulation. Similar orientations were recorded from televiewer logs run in wells 14-2 and 52-21 (Keys, 1979; Davatzes, 2016, written comm.) (refer to Fig. 2). The consistency of stress orientations in the wells indicates the direction of σ_{Hmax} is consistent across the region.

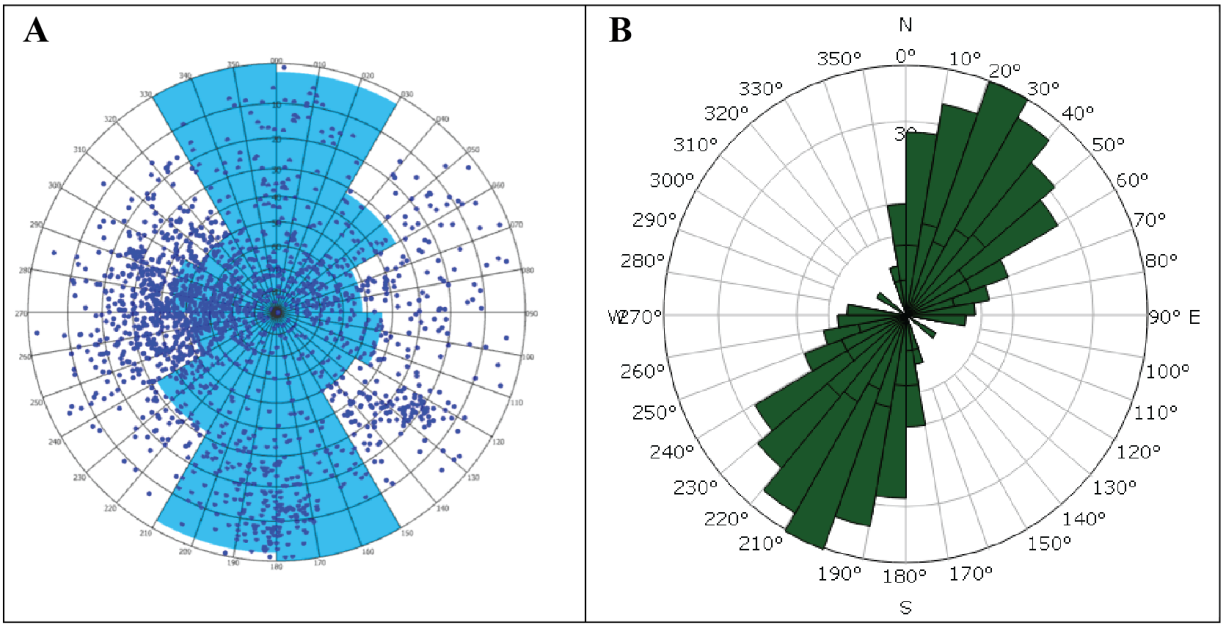

Figure 4. Orientations of fracture encountered in 58-32. A) Natural fractures. The majority of the fractures dip at moderate angles to the west (dark blue dots). The fractures strike NNW to NNE. Because the well is vertical, vertical fractures are underrepresented. B) Azimuths of induced fractures. The orientations of these fractures indicate that σ_{Hmax} trends NNE-SSW.

Injections have been carried out in three zones in well 58-32. The first injection program immediately followed completion of the well in 2017. This was in the barefoot section of the well. In 2019, this openhole section was re-stimulated and two uphole zones behind casing were perforated and separately tested. The 2017 stimulation was conducted to determine stress magnitudes and permeability in the 45 m (147 ft) of open hole below the 9 5/8-inch casing shoe. The testing consisted of an impulse test to assess permeability, three low-rate microhydraulic fracturing cycles for stress determination and a Diagnostic Fracture Injection Test (DFIT) at ~1431 L/min (~9 bpm) with an extended shut-in on September 22, 2017 (Fig. 5A). The testing continued on September 23, 2017 (Fig. 5B). Following a low rate injection cycle and a step rate test (SRT), 200-mesh calcium carbonate was pumped during injection at approximately~1431 L/min (~9 bpm). The purpose was to slightly prop the fractures taking fluid and to enhance differentiation between fractures identified in pre- and post- FMI logs. During the tests, a maximum injection rate of ~1431 L/min (~9 bpm) and a surface pressure of ~27.6 MPa (~4000 psig) was reached.

Stress gradients based on G-function analyses (measurements using the tangent and the compliance techniques for closure stress assessment) yielded a value of 14.0 kPa/m (0.62 psi/ft) for σ_{Hmin}. In the absence of analyzable breakouts, inflection changes on diagnostic plots and conventional breakdown calculations were used to constrain the maximum horizontal stress, σ_{Hmax}, as approximately 17.4 kPa/m (0.77 psi/ft). The gradient of the total vertical stress, σ_V was estimated to be 25.6 kPa/m (1.13 psi/ft) by integration of the density log from depth to the surface. These stress relationships are indicative of a normal faulting regime.

Comparison of the pre- and post- stimulation FMI logs from Sept 2017 demonstrates that significant enhancement and growth of the induced fractures occurred during the injection testing (Fig. 6). The orientations of these enhanced fractures confirm the NNE-SSW orientation of σ_{Hmax}. The low pressures applied during the injection tests provide prima facies evidence that reservoir conditions are appropriate for EGS development.

Permeability within the reservoir rocks is controlled by fractures. Transmissivity was determined from the first DFIT measurement to be 4.5 md-ft, suggesting a permeability of about 30 microdarcies.

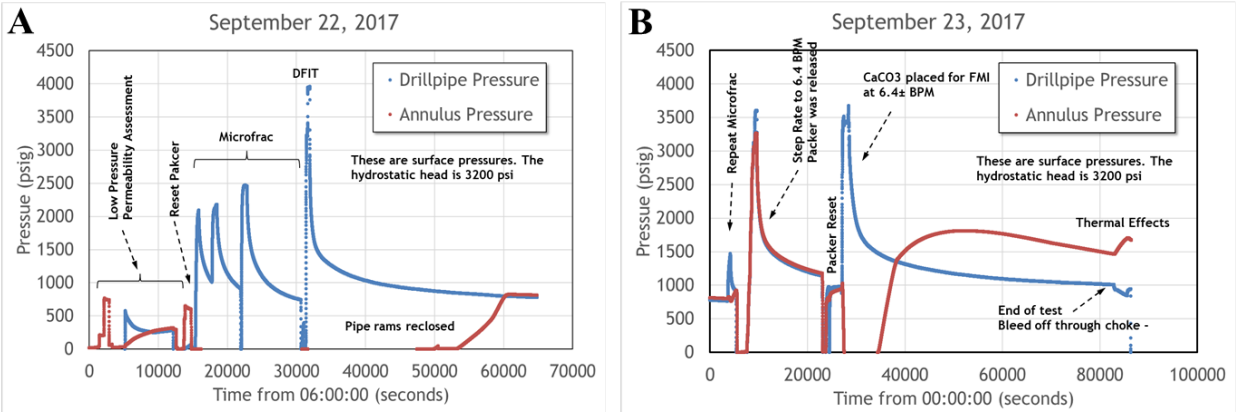

Figure 5. Surface pressures during the injection campaign. A) Injection program conducted on September 22, 2017. B) Injection program conducted on September 23, 2017. DFIT = Diagnostic Fracture Injection Test.

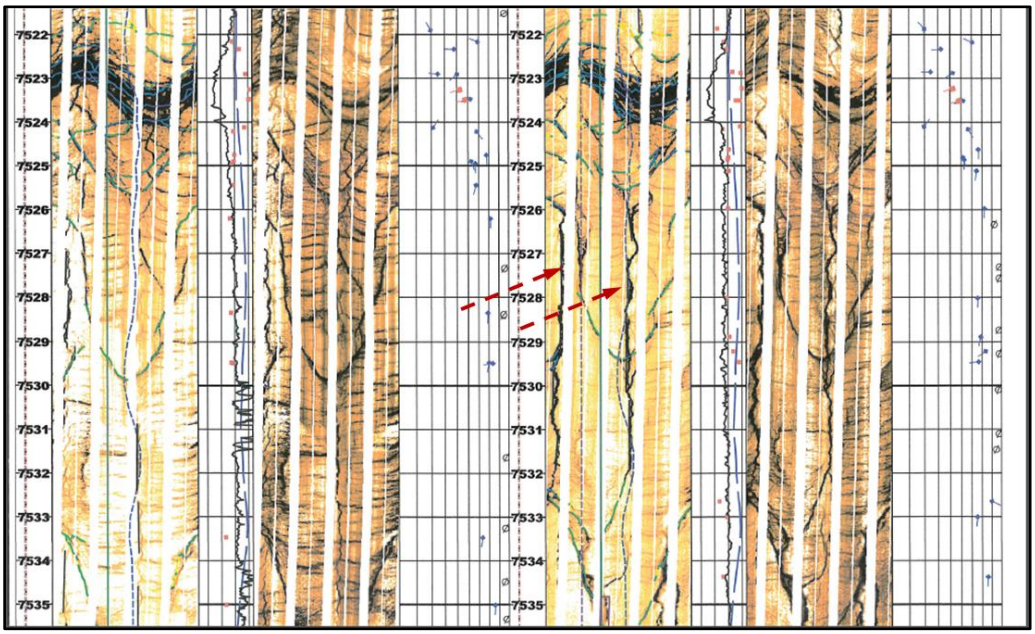

Figure 6. Comparison of FMI logs before (left two tracks) and after (right two tracks) injection. Induced fractures are near-vertical and are shown by circles with azimuth trends to the right of the tracks. Blue tadpole symbols show the direction and dip of natural fractures. The arrows point to induced fractures that display significant enhancement and growth after injection.

The sequence of injection testing in 2019 is shown in Table 1. The openhole testing program followed the 2017 test plan before increasing the injection rate to 2384.6 L/min (15 bpm). Similar injection rates were applied during the stimulations in the cased portion of the well. These injections were designed to determine the viability of stimulating fractures with different orientations behind casing. The lower perforated zone, between 2116-2129 m (6943-6953 ft) GL was located in a region of critically stressed fractures (fractures trending NNE parallel to σ_{Hmax}). Calculations suggested that these fractures would be the easiest to shear, dilate and propagate. Fig. 7a and b show the pressure response during cycles 4 and 5 respectively. Cycle 4 records the initial breakdown in this zone. The pressure response displayed in Fig. 5 indicates stimulation had already been initiated. The uppermost zone was perforated from 1995-1998 m (6544-6554 ft) GL contained a few fractures oriented at a high angle to σ_{Hmax} (noncritically stressed). It was assumed this zone would represent the upper limit of injection pressures required to stimulate the granitoid.

Table 1. Details of the 2019 injection testing program.

Zone	Ground level Depth (ft)	Cycle	Sub-desig	Maximum Tubing Pressure (psig)	Nominal Rate (bpm)	Total Volume (bbl)	Shut in tubing pressure (psig)	Closure Stress (psi)			Closure Stress Gradient (psi/ft)			Shut-in or Flowback	bbl	Volume Flowed Back (bbl)
1	7368-7515	1		1000	0.8	0.5		3908			0.53			Shut-in		
1	7368-7515	2		1166	0.8	1	1035	4120			0.56			Shut-in		
1	7368-7515	3		1377	2	1	1300	4192			0.56			Shut-in		
1	7368-7515	3	3A	1643	1.9	1	1371	-			-			Flowed Back	-	Too Small to Measure
1	7368-7515	3	3B	1487	2	1	1238	-			-			Flowed Back	-	Too Small to Measure
1	7368-7515	4		3955	5	30	2947	5802	5450	5200	0.77-0.78	0.73	0.7	Shut-in	18.79	After 15 hr and 36 minutes of shut-in 18.79 bbl were flowed back
1	7368-7515	5		3638	5	28	3060	5964	5253		0.8	0.71		Flowed Back	15.8	Flowed back for 1 hour and 39 minutes and recovered 15.8 bbl.
1	7368-7515	6	6	603	1	1	587				-			Shut-in	-	Flowed back after shut-in for78 minutes and then flowed back. Pressure built after shut-in.
1	7368-7515	6	6B	571	1	1	511	3623			0.49?			Shut-in	41	Pressure built after shut-in. After a 70 minute shut in, the well was flowed back.
1	7368-7515	7		3780	5.2	97	2770	5600	4700		0.75	0.63		Shut-in	5	After shut-in for 14 hours the choke was opened wide and 5 bbl were recovered.
1	7368-7515	7		3780	5.2	97	2770	6100	5650		0.82	0.76		Shut-in	5	Same cycle but stresses derived from back extrapolation of SRT. The previous data are for the first and second pressure humps.
1	7368-7515	7		3780	5.2	97	2770	6500	5920		0.88	0.8		Shut-in	5	Same cycle but stresses derived from another interpretation of the back extrapolation of the SRT. The previous data are for the first and second pressure humps.
1	7368-7515	7		3780	5.2	97	2770	5250			0.7			Shut-in	5	Same cycle but stresses derived from another interpretation of the back extrapolation of the SRT. The previous data are for the first and second pressure humps. These are the best SRT extrapolations because the data are friction-corrected (accounting for near-wellbore losses using the step down data.
1	7368-7515	8		4250	7.7		4213				0.57			Flowed Back	71	Flowed back for 3 hours to the rig tanks. Stress estimate is low quality.
1	7368-7515	9		5000	15	183	3639	5974			0.81			Shut-in		
2	6943-6953	1		1324	0.97	2	1227	4014			0.58			Shut-in	1.6	Flow back after shut-in over. Reopening estimated from leakoff behavior.
2	6943-6953	2		806	0.92	1	706	3706			0.53			Shut-in	1	After a one hour shut-in, the well was flowed back.
2	6943-6953	3	3											Shut-in		Bled down in 4 minutes and forty-five seconds.
2	6943-6953		3B	1060	1.8	1	892							Shut-in		
2	6943-6953	4		4182	5	32	3527	5974	3821		0.86	0.55		Shut-in		
2	6943-6953	5		4306	5	33		6382	5607		0.92	0.81-0.83		Flowed Back	17.6	Poor quality closure pick because the well was flowed back. Do not use it in analyses. However, the second stress is from the diagnostic plot and may be reasonable.
2	6943-6953	6		960	0.9	1	938	3747			0.54			Shut-in	3.2	Shut in for 170 minutes and then flowed back.
2	6943-6953	7		4525	5.1	190	2508	6650	5800		0.96	0.83		Flowed Back	105	From uncorrected SRT back-extrapolation.
2	6943-6953	7		4525	5.1	190	2508	6400	5650		0.92	0.81			105	Corrected for friction from SDT.
2	6943-6953	8		5023	9	110	4472	6684	5298		0.96	0.76		Shut-in	13	After 20 hours of shut-in the well was bled back to the pit and 13 bbl were recovered.
2	6943-6953	9		6818	15	188	6552	5900			0.9			Flowed back	90	Flowed back after 28 minutes of shut-in.
3	6544-6554	1		1306	0.75-1.0	2								Shut-in	1	The maximum pressure occurred during a water hammer on shut down, suggesting no fractures were taking fluid. The well was flowed back after shut-in.
3	6544-6554	2			0.8	1	840							Shut-in		
3	6544-6554	3		931	2	1	900							Shut-in		
3	6544-6554	4	4	6578	5	4.7	6578							Shut-in		
3	6544-6554	4	4A	6000	1-5	~7	6000									
3	6544-6554	4	4B	6677	3	~7.5	6677									
3	6544-6554	4	4C	6642	2.9	~5	6642									
3	6544-6554	4	4#6	6637	0.7	2.2	~6084	8685	8321		1.32	1.27				Broke over to 6450 psi. Either packer failure started or there may have been some initiation. The gradients have no obvious physical meaning.
3	6544-6554	5														Not pumped
3	6544-6554	6														Not pumped
3	6544-6554	7		6547	0.7-0.8		6698									Bridge plug failed
3	6544-6554	8														Bridge plug failed
3	6544-6554	9														

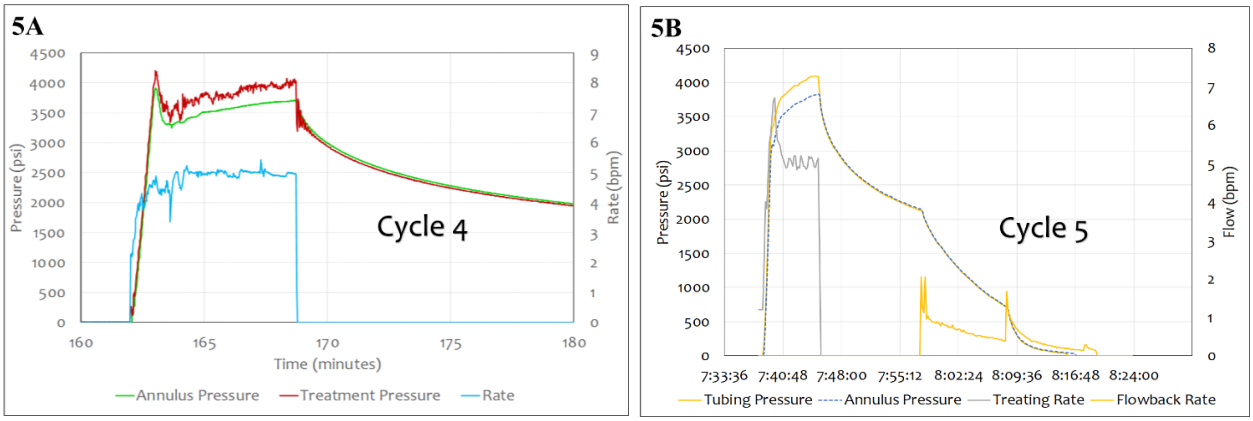

Figure 7. Examples of the pressure response during stimulation of critically stressed fractures. A) Cycle 4. The pressure response indicates the fractures were stimulated during this cycle. B) Cycle 5. The pressure response indicates the fractures had already failed. Notice that post-shutdown protocols were different for these two consecutive cycles. For cycle 4, the well was shut-in until the pressure had decayed. For cycle 5, a brief shut-in was followed by flowback through a 1/64-inch choke and later through a 2/64-inch choke.

6. MICROSEISMICITY

Microseismic activity during the injections was monitored at the surface with 5 seismometers and a nodal array of 150 nodes. A geophone and accelerometer was deployed in well 68-32 at a depth of ~282 m (925 ft) GL. Well 78-32 was instrumented with a Distributed Acoustic Sensing (DAS) cable and a 12-level string of geophones. The DAS cable was cemented in the annulus of the 5 ½ inch casing from 984 m (3228 ft) GL to the surface. The geophones were spaced 30 m (100 ft) apart between 645 and 981 m (2117 and 3217 ft) GL, straddling the alluvium-granitoid contact.

Prior to the stimulations, check shots were fired at two depths in well 58-32 (near TD and at 4000 ft MD) GL to assess the ability of detecting microseismic events. The check shots were observed on all in-well instruments. Four hundred twenty-three microseismic events were detected by the geophone string during the stimulations (Fig. 8). The DAS cable detected 43 events and the shallow instruments in well 68-32 detected 19 events. Five events were recorded by the nodal array.

The primary objective of the seismic monitoring was to demonstrate the utility of the monitoring tools in this environment. This objective was achieved in terms of event detection. As recognized before the testing, geometry of the monitoring wells (shallow) led to poorly constraining locations of the events. The apparent upward growth of the events to the west and the dispersed microseismic clouds are interpreted to be the result of monitoring bias and location uncertainties.

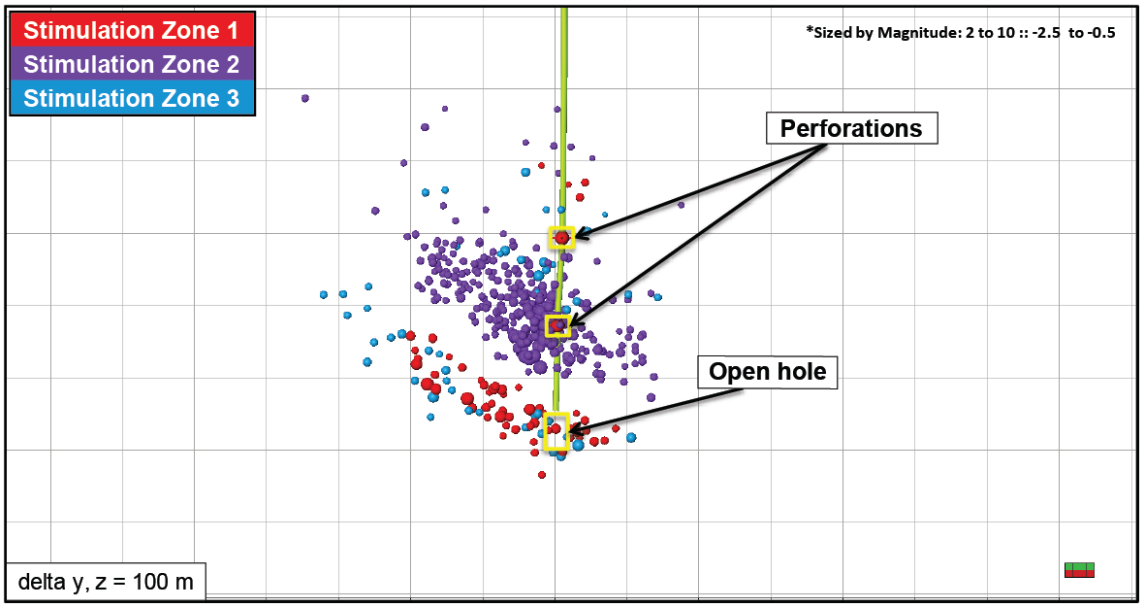

Figure 8. All events are colored according to the injection zone. Microseismic events recorded during pumping into Zone 1 (events associated with openhole injection at the bottom of the well) are shown as red circles. For Zone 2, with perforations from 2116-2129 m (6943-6953 ft) GL, events are shown in dark, royal blue. Microseismic events attributable to injection into Zone 3 (limited number of natural fractures or noncritically stressed fractures) are shown by circles colored light blue. The perforated depths for Zone 3 are 1995-1998 m (6544-6554 ft) GL. Note that most of the events associated with Zone 3 occurred in the lower zones because the bridge plug below the zone 3 perforations failed. Events identified west of the wellbore (away from the geophones) display upward growth away from the

targeted depths. This is interpreted to be the result of monitoring bias whereas the dispersed microseismic clouds can be attributed to location uncertainties.

Of the five isolation tools used in the 2019 injection program, four failed. Failure of the packers and/or bridge plug to effectively isolate sections of the well occurred during each of the stimulation sequences. The failure of the bridge plug during stimulation of the noncritically stressed fractures (Zone 3), led to a relatively small number of events near the upper perforation (Fig. 8). During treatment of Zone 3 after failure of the bridge plug, the abundance of microseismic events near the bottom of the well suggests that the bulk of the injected fluid entered fractures in the openhole section of the well and the lower perforated zone. Events are also present, although not as abundant, in the microseismic cloud formed during the stimulation of the zone with the critically stressed fractures.

7. CONCLUSIONS

The Milford FORGE site is ideally suited for the development and testing of technologies that can be used to create and sustain EGS reservoirs. The site is located adjacent to the Mineral Mountains. Data from nearly 100 deep and shallow wells, integrated with the results of new geologic mapping, and 2- and 3-D seismic reflection, gravity, and geochemical surveys, and the stimulation of well 58-32 has provided a detailed picture of the geological, thermal and stress characteristics of the FORGE reservoir.

Well 58-32 was drilled to a depth of 2297 m (7536 ft) KB on the FORGE site. The well penetrated 1329 m (4060 ft) of granitoid consisting primarily of granite, quartz monzonite and monzonite beneath the overlying gently dipping and undeformed alluvial deposits. The basement contact dips approximately 20º to the west across the FORGE site. A static temperature of 199ºC was measured at the base of the well. The top of the FORGE reservoir, defined by a temperature of 175ºC, was encountered at a depth of 1983 m (6507 ft) GL.

Induced fractures identified in the Formation Microscanner Image log of the well trend NNE-SSW, the direction of σ_{Hmax}. Stress gradients, determined from injection sequences conducted in the openhole section of well 58-32 in 2017 yielded values of 13.1-14.3 kPa/m (0.58-0.63 psi/ft) for σ_{Hmin} and 15.4-18.5 kPa (0.68-0.82 psi/ft) for σ_{Hmax}. A gradient of 25.6 kPa/m (1.13 psi/ft) was calculated for σ_V. Comparison of pre- and post-injection FMI logs documented enhancement and growth of the induced fractures, providing evidence that the stress field is appropriate for EGS development.

Three stimulations were conducted in 2019. The first stimulation was performed in the openhole section of the well. The second and third stimulations were designed to stimulate critically and noncritically stressed fractures behind casing. In the openhole section, injection performance mirrored the results of the 2017 testing. Injection occurred at even lower pressures than had been experienced in 2017, suggesting some degree of permanence of the fracture system. Multiple closure stress signatures suggest closure of tensile fractures and dilated natural fractures. The formation readily took fluid at modest injection rates 2384.6 L/min (15 bpm) suggesting upscaled stimulation activities should be feasible in Phase 3 of this program, where extended reach wells will be interconnected hydraulically. The lower cased and perforated zone was successfully treated. The zone with the critically stressed fractures broke down at a surface pressure of 29 MPa (4200 psig) at an injection rate of 795 L/min (5 bpm). The pressure signature was completely consistent with tensile failure along the axis of the wellbore or the reactivation of an inclined, cemented, natural fracture. Again, the formation took fluid at 2384.6 L/min (15 bpm) down casing at a manageable surface treatment pressure of approximately 44.8 MPa (6500 psi) down 3 1/2-inch tubing (much higher rates will be achievable down casing). The zone with noncritically stressed fractures was much more difficult to breakdown. It may have experienced some fracture initiation at ~45.5 MPa (~6600 psig). This was the limit of the wellhead. The packer had failed – otherwise pressure could have been increased to just under 55.2 MPa (8,000 psi). This strongly indicates the importance of engineered rather than geometric completions or alternatively, implementation of creative initiation procedures. More than 420 microseismic events were recorded on a 12-level geophone string that straddled the alluvium-granitoid contact. The tests confirm earlier results indicating the granitoid is an ideal host for an EGS reservoir.

ACKNOWLEDGEMENTS

Funding for this work was provided by U.S. DOE under grant DE-EE0007080 “Enhanced Geothermal System Concept Testing and Development at the Milford City, Utah FORGE Site”. We thank the many stakeholders who are supporting this project, including Smithfield, Utah School and Institutional Trust Lands Administration, and Beaver County. A grant from the Utah Governor’s Office of Energy Development has provided support for educational outreach activities. The Bureau of Land Management and the Utah State Engineer’s Office have been very helpful in guiding the project through the permitting processes. We are especially grateful for the field support provided by Virgil Welch, Duane Winkler, and Mary Mann. Gosia Skowron assisted in the preparation of the figures and manuscript. Her help is greatly appreciated.

REFERENCES

Allis R.G., and Larsen, G.: Roosevelt Hot Springs Geothermal field, Utah – reservoir response after more than 25 years of power production, *Proceedings*, 37th Workshop on Geothermal Reservoir Engineering, Stanford University, Stanford, CA (2012).

Allis, R., and Moore, J.N., eds.: Geothermal Characteristics of the Roosevelt Hot Springs System and Adjacent FORGE EGS Site, Milford Utah, *Utah Geological Survey Miscellaneous Publication* **169**, (in press).

Aleinikoff, J.N., Nielson, D.L., Hedge, C.E., and Evans, S.H.: Geochronology of Precambrian and Tertiary rocks in the Mineral Mountains, south-central Utah, *US Geological Survey Bulletin*, **1622**, (1987), 1-12.

Bartley, J.M.: Joint patterns in the Mineral Mountains intrusive complex and their roles in subsequent deformation and magmatism *in* Allis, R. and Moore, J.N., eds. Geothermal Characteristics of the Roosevelt Hot Springs System and Adjacent FORGE EGS Site, Milford Utah, *Utah Geological Survey Miscellaneous Publication* **169**, (in press).

Coleman, D.S. and Walker, J.D.: Evidence for the generation of juvenile granitic crust during continental extension, Mineral Mountains Batholith, Utah, *Journal of Geophysical Research*, **97**, (1992), 11011-11024.

Dickinson, W.R.: Geotectonic evolutions of the Great Basin, *Geosphere*, **2**, (2006), 353-368.

Gwynn, M., Allis, R., Hardwick, C., Jones, C., Nielsen, P., Hurlbut, W.: Rock properties of FORGE well 58-32, Milford, Utah, *Transactions Geothermal Resources Council*, **42**, (2018).

Hardwick, C.L., Hurlbut, W., Gwynn, M., Allis, R., Wannamaker, P., and Moore, J.: Geophysical surveys of the Milford, Utah FORGE Site: Gravity and TEM, *Transactions Geothermal Resources Council*, **42**, (2018).

Hardwick, C.L., Gwynn, M., Allis, R., Wannamaker, P., and Moore, J., 2016, Geophysical Signatures of the Milford, Utah FORGE Site *Proceedings*, 41th Workshop on Geothermal Reservoir Engineering, Stanford University, Stanford, CA (2016).

Hintze, L.F., and Davis, F.D.: Geology of Millard County, Utah, *UGS Bulletin*, **133**, (2003), 305.

Keys, W. S.: Borehole geophysics in igneous and metamorphic rocks, *Transactions*, 20th Society of Professional Well Log Analysts Annual Logging Symposium, Tulsa, Oklahoma, (1979), 001-026.

Kirby, S.M., Knudsen, T.R., Kleber, E., and Hiscock, A.: Geologic map of the Utah FORGE Area: Utah Geological Survey Contract Deliverable for DOE project number DE-EE0007080, scale 1:24,000, 2 plates, (2018a), 13.

Kirby, S.M., Knudsen, T.R., Kleber, E., and Hiscock, A.: Geologic setting of the Utah FORGE site, based on new and revised geologic mapping, *Transactions Geothermal Resources Council*, **42**, (2018b).

Kleber, E., Hiscock, A., Kirby, S., Allis, R., Quirk, B.: Assessment of Quaternary faulting near the Utah FORGE site from high resolution topographic data, *Transactions Geothermal Resources Council*, **41**, (2017).

Jones, C.G., Moore, J.N., and Simmons, S.F.: Lithology and Mineralogy of the Utah FORGE EGS Reservoir: Beaver County, Utah, *Transactions Geothermal Resources Council*, **42**, (2018).

Miller, J., Allis, R., and Hardwick, C.: Seismic reflection profiling at the FORGE Utah EGS site, *Transactions Geothermal Resources Council*, **42**, (2018).

Miller, J., Allis, R., and Hardwick, C.: Interpretation of seismic reflection surveys near the FORGE Enhanced Geothermal Systems site, Utah *in* Allis, R. and Moore, J.N., eds. Geothermal Characteristics of the Roosevelt Hot Springs System and Adjacent FORGE EGS Site, Milford Utah, *Utah Geological Survey Miscellaneous Publication* **169**, (in press).

Nielson, D.L., Evans, S.H., and Sibbett, B.S.: Magmatic, structural, and hydrothermal evolution of the Mineral Mountains intrusive complex, Utah, *Geological Society of America Bulletin*, **97**, (1986), 765-777.

Welsh, J. E.: McCulloch Acord 1-26, Roosevelt Hot Springs Area, Beaver Co., Utah. Unpublished petrography (1980).

Zandt, G., McPherson, L., Schaff, S., and Olsen, S.: Seismic baseline and induction studies: Roosevelt Hot Springs, Utah and Raft River, Idaho, *U.S. Dept. of Energy Report DOE 01821-T1*, (1982), 58.